

Therapeutic Mitochondrial Delivery to Astrocytes for Ischemic Stroke

A Technical Report submitted to the Department of Biomedical Engineering

Presented to the Faculty of the School of Engineering and Applied Science
University of Virginia • Charlottesville, Virginia

In Partial Fulfillment of the Requirements for the Degree
Bachelor of Science, School of Engineering

Caitleen Copeland
Spring, 2020

Technical Project Team Members
Emma Taylor-Fishwick

On my honor as a University Student, I have neither given nor received
unauthorized aid on this assignment as defined by the Honor Guidelines
for Thesis-Related Assignments

Therapeutic Mitochondrial Delivery to Astrocytes for Ischemic Stroke

Caitleen A. Copeland^{a,*}, Emma C. Taylor-Fishwick^{a,*}, Catherine M. Gorick^a, Richard J. Price^{a,1}

^a Biomedical Engineering, University of Virginia

¹ Correspondence: RJC

Email: rprice@virginia.edu

Address: Box 800759, Health System, Charlottesville, VA 22908

Phone: 434-924-0020

* Authors contributed equally on this work

Abstract

Ischemic stroke is caused by a blood clot lodged in an artery supplying blood to the brain and is a leading cause of death in the US. Although there are treatments to remove the clot and replenish blood flow to the brain, current treatments do not address the damage to mitochondria that occurs as a result of an ischemic stroke. The dysfunctional mitochondria are transferred from astrocytes to neurons, continuing the ischemic cascade and leading to further post-stroke complication and disabilities. Transfer of mitochondria has been seen to improve myocardial function in patients with myocardial ischemia reperfusion injury. Therefore, the goal of this project was to determine which tissue source (cardiac muscle, skeletal muscle, or adipose tissue) provides the most effective mitochondria for maximum uptake and ATP production in astrocytes. Cardiac mitochondria were found to have significantly higher ATP production per mitochondria than all other types of mitochondria when not in cells. When mitochondria were added to astrocytes, peridroplet adipose mitochondria exhibited the highest ATP production in astrocytes at a quantity that was significantly higher than cardiac and cytoplasmic adipose mitochondria. Skeletal mitochondria were found to have the highest uptake in astrocytes at a significantly higher rate than all other types of mitochondria, but all types were uptaken at a high level. Based on these results, peridroplet adipose mitochondria had the highest ATP production in astrocytes, high uptake in astrocytes, and adipose tissue provided the quickest removal that would have the shortest recovery time in human patients. Therefore, peridroplet adipose mitochondria was determined to be the most effective therapeutic for treatment of ischemic stroke in order to decrease mitochondrial dysfunction and post-stroke complications in patients.

Keywords: Ischemic Stroke, Astrocytes, Cardiac Mitochondria, Skeletal Mitochondria, Peridroplet and Cytoplasmic Adipose Mitochondria

Introduction

Stroke is the leading cause of physical and intellectual disability and has a high rate of mortality in many developed countries around the world, including the US¹. Approximately 795,000 people per year, in the US, have a new or recurrent stroke, and of these 87% are classified as ischemic stroke caused by a blood clot lodged in an artery supplying blood to the brain². For patients that do have an ischemic stroke, the lifetime costs are great. In 2004, it was estimated that the indirect and direct costs of stroke exceeded 53 billion dollars. Additionally, it is estimated that between 2005 to 2050, this cost will exceed 2.2 trillion dollars³.

The current standard of treatment for ischemic stroke involves an intravenous injection of recombinant tissue plasminogen activator (rt-PA)⁴. The rt-PA works by breaking down the blockage in order to restore blood flow⁵. However, with this treatment, more than half of patients do not recover fully. A new treatment, endovascular therapy, involves using an intra-arterial thrombolysis with t-PA, a mechanical clot remover, or a combination of the two. However, when the two treatments were compared, it was found that the endovascular therapy had a 4.4% lower rate of disability-free survival⁴. This therefore shows that there is a lack of treatment approaches that are broadly effective at reducing the disability rate after an ischemic stroke. A potential reason for this is the fact that none of the current treatments address the mitochondria that become dysfunctional after an ischemic stroke.

After an ischemic stroke, mitochondria become dysfunctional due to oxygen and glucose deprivation⁶. In healthy brain tissue, astrocytes transfer mitochondria particles to the neurons via the calcium-dependent mechanisms of CD38 and the cyclin adenosine diphosphate (ADP) ribose signaling^{7,8}. These mechanisms allow for cell-to-cell communication between astrocytes and neurons and increases adenosine triphosphate (ATP) production and the viability of the neurons⁴. However, when these mitochondria become dysfunctional (as in ischemic stroke) they have abnormalities in mitochondrial membrane potential, produce increased amounts of reactive oxygen species (ROS), and display decreased ATP production⁶. As a result, when these dysfunctional mitochondria are passed from astrocytes to neurons, they continue the ischemic cascade and therefore lead to decreased neuronal viability and potentially increased post-stroke complications.

Approximately 85% of stroke patients have complications during their hospital admission. Additionally, follow-up complications after leaving the hospital include infections, falls with serious injury, blackouts, pains, and symptoms of depression and anxiety⁹. Thus, several patients have an associated lower quality of life, and a number of people are unable to work or receive financial assistance after having a stroke¹⁰. This high rate of complications and low quality of life following ischemic stroke indicates that an improved therapeutic method is needed. Therefore, creating a treatment for ischemic stroke that addresses the dysfunctional mitochondria and limits the downward cascade could be vital for

reducing the number of patients who have to live with disabilities following an ischemic stroke.

There has been previous work within the field to investigate the use of mitochondrial transplantation for the treatment of ischemia-reperfusion injuries. In a clinical study, transplantation of mitochondria improved myocardial function within 24 to 48 hours after treatment in pediatric patients with myocardial ischemia reperfusion injury following coronary artery occlusion and revascularization¹¹. This study suggests that the delivery of functional mitochondria can help to reverse the effects of ischemia-reperfusion injury, such as in the context of stroke.

The effects of mitochondrial transplantation have also been studied in the context of stroke. The first of these studies was completed by Po-Jui Huang and his colleagues. The study demonstrated that the transfer of exogenous mitochondria via in-situ injection or systemic administration mitigated cell death in both middle cerebral artery occlusion (MCAO) rats and oxygen-glucose deprived (OGD) neurons, which represent in vivo and in vitro stroke models, respectively¹². Additionally, motor function of the MCAO rats was improved following mitochondrial treatment.

Another study investigated the therapeutic role of astrocytes in stroke recovery. Cultured astrocytes were observed to produce functional extracellular mitochondria, which are able to increase the ATP levels and viability of neurons that have suffered an OGD injury. Additionally, the transplantation of mitochondria to the peri-infarct cortex of MCAO mice resulted in an upregulation of cell-survival-related signals¹³. This study indicates that astrocytes have the ability to transfer healthy mitochondria to rescue damaged neurons after stroke due to cell-to-cell communication.

Although these studies demonstrated that exogenous mitochondria have potential as a therapeutic for damaged neurons as a result of ischemic stroke, the effect of using mitochondria from different tissue sources was not investigated. Previous studies have shown that different types of mitochondria vary in some properties. Cytoplasmic mitochondria are typically found in skeletal muscle and most tissue sources, and they are the basis of the mitochondrial studies detailed above. Peridroplet mitochondria from adipose tissue have enhanced bioenergetics (ATP synthesis, electron transport capacities, oxidative phosphorylation capacity), low fatty acid oxidation capacity, and fusion-fission properties that differentiate them from cytoplasmic mitochondria¹⁴. Myocardium mitochondria, extracted from cardiac muscle, have a larger reliance on aerobic ATP as compared to skeletal muscle mitochondria¹⁵. Additionally, cardiac and skeletal muscle mitochondria have similar oxidative phosphorylation capacities but vary in terms of respiratory control rate and nonphosphorylating respiration¹⁶.

The underlying differences among mitochondria from different tissues postulates that mitochondria from different sources have varying ATP production and uptake potential. Therefore, this project aims to design a therapeutic method that meets the following design criteria. In order for the therapeutic to be successful, the tissue and mitochondria extraction must occur within a few hours, the surgery must have minimal recovery time, and the determined mitochondria must have high uptake and ATP production in astrocytes. The mitochondria that is determined to meet the most design criteria has the potential to provide the most effective, novel therapy to treat dysfunctional mitochondria associated with ischemic stroke.

Materials and Methods

Tissue harvest

All tissues used for experimentation were harvested from mice. To harvest tissue, the mouse was first anesthetized with an intraperitoneal injection of 120 mg/kg ketamine, 12 mg/kg xylazine, and 0.08 mg/kg atropine in a sterilized 0.9% saline. The mouse was then shaved in any

area where the tissue was to be harvested, and surgery was conducted. Skeletal muscle was harvested from the hindlimb, brown adipose tissue was harvested from fat deposits between the shoulder blades, and the heart was removed for cardiac muscle. The mouse was sacrificed by cardiac perfusion with 10 ml ice cold PBS. This protocol was repeated for multiple mice for each experiment.

Skeletal and cardiac muscle mitochondria extraction

To extract mitochondria from skeletal and cardiac muscle, Thermo Scientific's Mitochondria Isolation Kit for Tissue was used. The accompanied Reagent-based Method for Soft Tissues protocol was followed for these tissues. Skeletal and cardiac muscle were kept separate throughout the protocol. First, the tissues were homogenized using the Miltenyi gentlemacs dissociator. After homogenization, the mitochondria were isolated through centrifugation, vortexing, and the addition of kit supplied reagents as described in the kit protocol as shown in the first two sequences of Figure 1. The final product was one pellet of mitochondria for each type of mitochondria (skeletal and cardiac) per mouse that was harvested.

Cytoplasmic and peridroplet mitochondria extraction from adipose tissue

In order to extract peridroplet and cytoplasmic mitochondria from adipose tissue acquired through tissue harvest, a combination of the Thermo Scientific's Mitochondria Isolation Kit for Tissue Protocol and the protocol for *Cytoplasmic and Peridroplet Mitochondria found in the appendix of Mitochondria Bound to Lipid Droplets Have Unique Bioenergetics, Composition, and Dynamics that Support Lipid Droplet Expansion* was used¹⁴. The adipose tissue was first homogenized using the Miltenyi gentlemacs dissociator. The homogenized solution was then centrifuged at low speed (900 g) in order to separate the fat in the adipose tissue from the rest of the solution. The fat and supernatant were then separated into two separate conical tubes. From this point on, the fat was processed for peridroplet mitochondria and the supernatant was processed for cytoplasmic mitochondria using reagents from the Thermo Scientific Mitochondria Isolation Kit as shown in the third sequence of Figure 1. One pellet was obtained for each type of mitochondria for each mouse that was harvested.

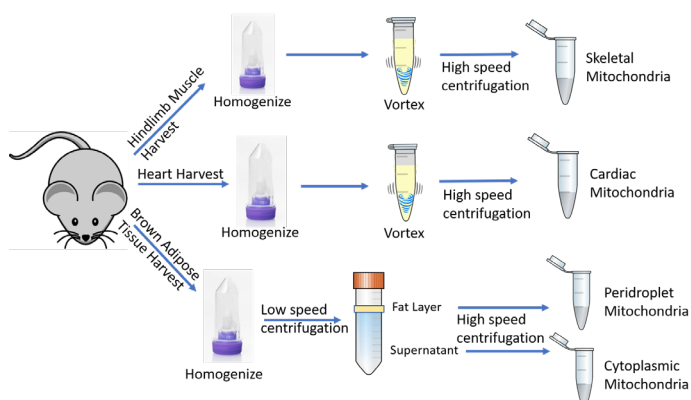


Fig. 1. Methods of Mitochondria Extraction. The extraction methods for mitochondria from the three chosen tissue sources. The first two sequences had the same extraction method to extract skeletal and cardiac mitochondria from hindlimb muscle and the heart, respectively. The third sequence shows the extraction method for peridroplet and cytoplasmic mitochondria from brown adipose tissue.

Mitochondria staining

Once the final mitochondria pellets were obtained, 1 μ L of MitoTracker stock solution was added to each pellet. The pellets were then incubated at 37°C for 30 minutes. After incubation, the pellets were centrifuged at 12,000 g for 5 minutes. The remaining stain was then removed, and the pellets were resuspended in 1 mL of PBS.

ATP production measurement of mitochondria in astrocytes

The day before experimentation, astrocytes were seeded at a density of 2e4 cells/well in up to 60 wells of a 96 well plate, depending on the amount of astrocytes available. On the day of experimentation, unstained mitochondria were added to the wells containing astrocytes and ~3 wells containing astrocytes were not given mitochondria. The plate was then incubated for 1.5 hours at 37 °C. After incubation, the plate was rinsed three times with PBS to remove any mitochondria that were not uptaken. After rinsing, all wells were filled to a volume of 100 μ L of PBS. Additionally, one column of wells, not containing astrocytes, were given 100 μ L of unstained mitochondria and another empty column was given 100 μ L of stained mitochondria (2 samples per mitochondria type). 100 μ L of Cell-Titer Glow ® was then added to all wells that contained astrocytes and mitochondria except eight (two per type of mitochondria) and to the three wells containing astrocytes alone. Additionally, the column of unstained mitochondria alone was given 100 μ L Cell-Titer Glow ®. The plate was then mixed and incubated at room temperature. Then, the plates were read on a SpectraMax Id3 microplate reader for luminescence, and the column of stained mitochondria was read for fluorescence.

Uptake measurement of mitochondria in astrocytes

The day before experimentation astrocytes were seeded at a density of 2e4 cells/well in up to 60 wells of a 96 well plate depending on the amount of astrocytes available. Stained mitochondria were added to the astrocyte wells of the plate except ~3 wells. The plate was then incubated for 1.5 hours at 37 °C. After incubation, the plate was rinsed three times with PBS to remove any mitochondria that were not uptaken. After rinsing, all wells were filled to a volume of 100 μ L of PBS. Additionally, one column of wells not containing astrocytes were given 100 μ L of unstained mitochondria and another empty column was given 100 μ L of stained mitochondria (2 samples per mitochondria type). The column of unstained mitochondria alone was given 100 μ L Cell-Titer Glow ®. The plate was then mixed and incubated at room temperature. Then, the plate was read on a SpectraMax Id3 microplate reader for fluorescence and the column containing unstained mitochondria was read for luminescence.

Confocal confirmation of mitochondria uptake

Confocal microscopy was used to confirm that the stained mitochondria quantified from the fluorescence plate reader actually were uptaken into astrocytes. Astrocytes were plated in 18 wells of an Ibidi 24 well μ -plate the night before experimentation at a seeding density of 3.5e4 cells/well. The morning of experimentation, 300 μ L of each type of stained mitochondria were added to 12 of the wells containing astrocytes (4 wells per type of mitochondria), and the plate was incubated at 37°C overnight. The next morning, all 18 wells containing cells were stained for glial fibrillary acidic protein (GFAP), which represents the astrocyte cytoskeleton, and DRAQ5, which represents nuclei. Following staining, z-stack images of the wells were taken on the Nikon Eclipse TE2000 confocal microscope equipped with a 63x oil objective.

Mitochondria diameter measurement

To test the relative size of each type of mitochondria, two pellets of each type of extracted mitochondria were suspended in 1 mL of deionized water. This was repeated for each type of mitochondria in order to obtain two solutions for each type. The eight solutions were then analyzed on a Zetasizer Nano S90 three times in order to ensure consistency in the results. The samples were then diluted by 50% with deionized water and run again three times.

Results

Mitochondria from different tissue sources vary in particle size

In order to determine the size of the different types of mitochondria, the *Mitochondria diameter measurement* procedure described in the methods section was followed. The values, from the diluted samples, were consistent with the values from the non-diluted samples. Therefore, the diluted and undiluted sample z-ave values were combined and the average and standard deviation were computed for each type of mitochondria as shown in Figure 2. The z-ave value from the Zetasizer Nano S90 is the preferred dynamic light scattering (DLS) parameter which relates to particle diameter.

As demonstrated in Figure 2, cytoplasmic mitochondria, from adipose tissue, were seen to have the largest diameter while skeletal and peridroplet diameters were smaller. A one-way ANOVA with Tukey's post hoc test was run on the data to confirm these observations following New England Journal of Medicine (NEJM) style. All types of mitochondria were found to be significantly different ($p < 0.5$) from each other except for skeletal and peridroplet.

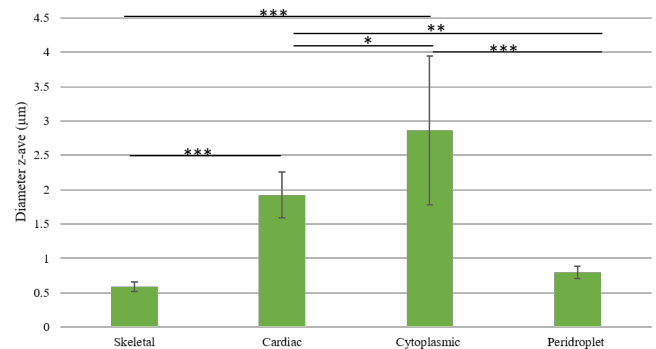


Fig. 2. Mitochondria Diameter. Diameter results for each type of mitochondria based off of zetasizer analysis. Each bar represents the average of all z-ave results for that mitochondria type. The diameter of all mitochondria types was significantly different with the exception of skeletal and peridroplet which had no significant difference in size. The statistical results are reported following New England Journal of Medicine (NEJM) style.

ATP production per mitochondria varies depending on the type of mitochondria

To compare the inherent ATP production of each type of mitochondria outside of cells, the average ATP production per mitochondria was determined. Controls of stained and unstained mitochondria alone were added to every ATP production and uptake experiment as described in the methods section. The average luminescence value, which represents ATP production, was divided by the average fluorescence value, representing quantity of mitochondria, for each type of mitochondria for each of the six experiments conducted (3 ATP production plates and 3 uptake plates). The average for the six experiments was then computed

to calculate the overall average ATP production for each type of mitochondria and is shown in Figure 3.

The average ATP production per mitochondria was highest for cardiac mitochondria with it being significantly larger than both cytoplasmic and peridroplet mitochondria according to a one-way ANOVA with a Tukey's post hoc test ($p < 0.5$). However, cardiac mitochondria also had the highest standard deviation, which is due to the sample size being small ($n=6$) and also due to the mice, from which the tissue is extracted, being of varying age.

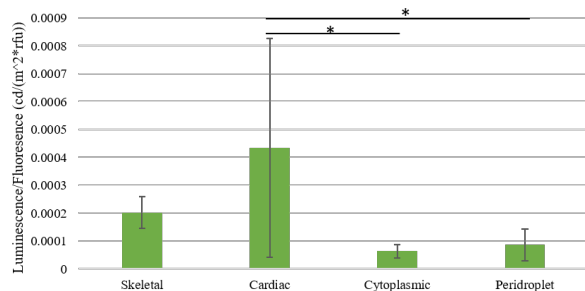


Fig. 3. Average ATP Production per Mitochondria. The ATP production per mitochondria was determined by dividing the luminescence of mitochondria alone by the fluorescence of those mitochondria alone. Mitochondria in cardiac muscle produced the greatest amount of ATP per mitochondria but also had a high standard deviation. The statistical results are reported following New England Journal of Medicine (NEJM) style. Cardiac mitochondria were significantly different from cytoplasmic and peridroplet mitochondria.

Mitochondria type affects ATP production in astrocytes

Three replicates of the ATP production measurement of mitochondria in astrocytes as described in the methods section were conducted. The luminescence value of astrocytes alone was subtracted from the luminescence value of astrocytes that were administered mitochondria treatment. This value was then normalized to the fluorescence of mitochondria alone, a control added to every replicate that represents the quantity of mitochondria in each sample. Between the three replicates, batch effects were observed. To correct for this, all data, within each replicate, was normalized to the average peridroplet value from that replicate. All three replicates were then combined and the results are shown in Figure 4.

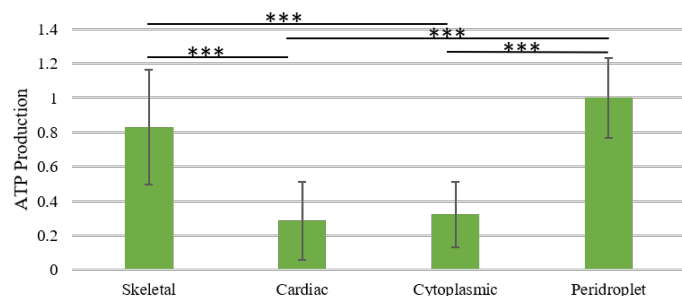


Fig. 4. ATP Production in Astrocytes. ATP production of each type of mitochondria, in astrocytes, is based off of luminescence values from an ATP reagent. The data was normalized to fluorescence of the mitochondria alone and to the average peridroplet value for each replicate. The statistical results are reported following NEJM style. Skeletal and peridroplet mitochondria were determined to be significantly different from cardiac and cytoplasmic mitochondria.

A one-way ANOVA with a Tukey's post hoc test was used to analyze the data. Peridroplet mitochondria was seen to have the highest ATP production in astrocytes. Additionally, both peridroplet and skeletal mitochondria had ATP production in astrocytes that was significantly higher than that of cardiac and cytoplasmic mitochondria ($p < 0.001$).

Astrocytes uptake mitochondria of different types at varying rates

Three trials of the Uptake measurement of mitochondria in astrocytes were conducted as described previously. The fluorescence value of astrocytes alone was subtracted from the fluorescence value of astrocytes that were given stained mitochondria. These values were then normalized to the fluorescence value of the mitochondria alone. Additionally, batch effects were again observed and were corrected by normalizing the data to the peridroplet data of each replicate as done for the ATP production in astrocytes data. The normalized average value for uptake of each type of mitochondria is shown in Figure 5.

Skeletal mitochondria were seen to have been uptaken in astrocytes at a significantly higher rate than all other types of mitochondria according to a one-way ANOVA with Tukey post-hoc test. The results of the ANOVA with Tukey post-hoc test are illustrated in Figure 5 and follow the NEJM style. However, all other types of mitochondria were still uptaken at a substantial rate by the astrocytes.

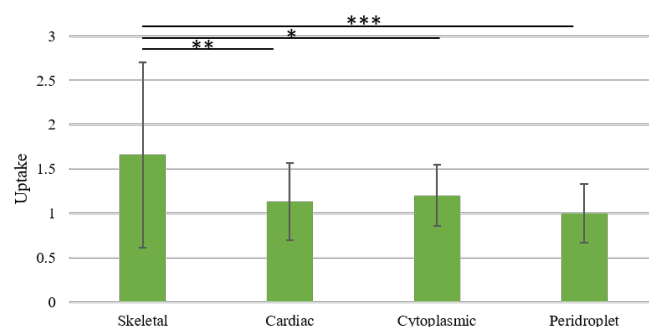


Fig. 5. Uptake in Astrocytes. Uptake of each type of mitochondria, in astrocytes, is based off of the fluorescence of stained mitochondria. The data was normalized to fluorescence of the mitochondria alone and to the average peridroplet value for each replicate. The statistical results are reported following NEJM style. Skeletal mitochondria were determined to be significantly different from cardiac, cytoplasmic, and peridroplet mitochondria.

Mitochondria are fully uptaken by astrocytes

To confirm that the added mitochondria were fully uptaken into the astrocytes in experimentation, z-stack images were taken of each type of mitochondria in astrocytes as described in the *Confocal confirmation of mitochondria uptake* section of the methods. Representative z-stack projections (z-stacks compressed into a single 2D image) are shown for each type of mitochondria in Figure 6A. The images clearly demonstrate the overlap between stained mitochondria (red) and stained astrocytes (green) confirming that the mitochondria were uptaken into the cells. It was further confirmed that the mitochondria were fully uptaken into the astrocytes by confirming an overlap between the mitochondria and astrocyte stains on every slice of each z-stack. A representative series of the z-stack slices for the cytoplasmic mitochondria is shown in Figure 6B. The images demonstrate a clear overlap between the stains throughout the z axis of the cell confirming that the mitochondria

completely entered the cell.

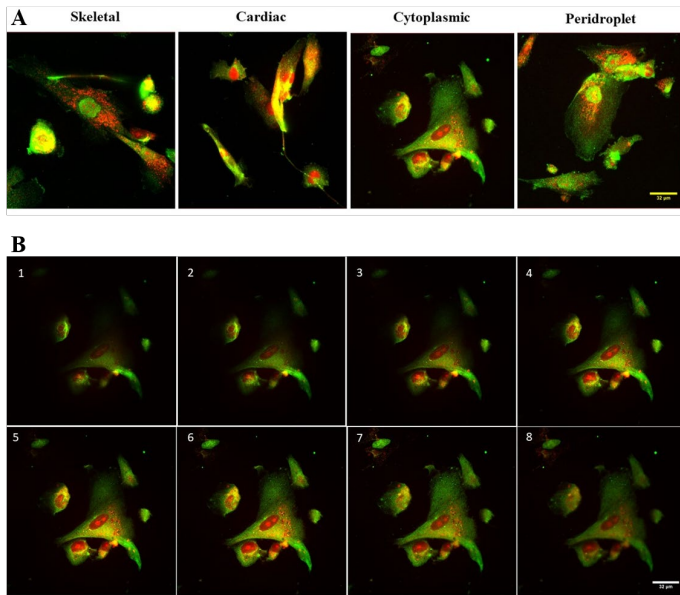


Fig. 6. Confocal z-stacks of Uptaken Mitochondria in Astrocytes. The red stain represents the expression of MitoTracker™ stained mitochondria. The green stain represents the expression of Glial Fibrillary Acidic Protein (GFAP). **A)** Representative z-stack projections of the overlap between each type of mitochondria and astrocytes. **B)** Series of slices from the z-stack of the cytoplasmic mitochondria. In each slice, there is an overlap between the mitochondria and astrocyte stains demonstrating that the mitochondria are fully uptaken into the cell.

Discussion

Peridroplet mitochondria is the best therapeutic option for treatment of ischemic stroke

Peridroplet mitochondria met all of the design criteria and therefore would be the best type of mitochondria to be used as a therapeutic treatment for ischemic stroke. Out of the three tissue sources, the extraction of adipose tissue from mice was the fastest and also least invasive, therefore leading to the surgery having the shortest recovery time. Thus, based on the first two criteria, treatment feasible in a short time frame and minimal recovery time, the mitochondria from adipose tissue, peridroplet and cytoplasmic, would be the most optimal for a treatment. Additionally, cytoplasmic and peridroplet mitochondria were both substantially uptaken by astrocytes, and therefore satisfied the third criteria (Figure 5). Peridroplet mitochondria, however, had a significantly higher ATP production in astrocytes compared to cytoplasmic, therefore satisfying the fourth and most important design criteria (Figure 4). This is because ATP production is a key metric in understanding the function of the mitochondria in astrocytes and is needed to be high in order to replenish the ATP due to dysfunctional mitochondria producing a low quantity of ATP. Therefore, based on all the results, peridroplet mitochondria are the best option for the most effective therapeutic.

Limitations

There were several limitations in our experimentation which caused variability in our data. First, there were obstacles in resuspending the

mitochondrial pellets into a homogenous solution, as the mitochondrial pellets were often hard to break up. Additionally, there was no way of determining if the mitochondria and PBS were a homogenous solution. This therefore led to inconsistencies in regards to the quantity of mitochondria that were being added to each well and also explains the high standard deviations that were seen throughout the experimentation. Furthermore, the data of most of our experiment was normalized to fluorescence of mitochondria alone to represent the quantity of mitochondria in each sample. However, this was not an exact metric to compare the quantity of mitochondria and was subject to the same variability of our treatment samples.

Another limitation was that although we followed established protocols to separate peridroplet and cytoplasmic mitochondria from adipose tissue, we did not confirm that the populations we found were pure and distinct. Therefore, it is possible that there was contamination of peridroplet mitochondria in the cytoplasmic mitochondria and vice versa. However, we believe that the contamination, if any, would be very limited and therefore would not cause a huge alteration in our results.

A third limitation of our experimentation is that the mice used for our experiment were of varying ages. Previous studies have found that the age and fitness level have a large effect on the bioenergetics and functionality of mitochondria¹⁷. This could explain the high standard deviation shown in regard to ATP production of cardiac mitochondria outside of astrocytes, as tissues of high-energy demand, such as the heart, have been particularly shown to become dysfunctional with age (Figure 3)¹⁷.

Future directions

The data presented is based off of a limited number of data points, especially in regards to the data for ATP production per mitochondria. Therefore, more replicates of the experiments are needed to confirm our findings. Furthermore, our data for ATP production and uptake in astrocytes were subject to batch effects. It is probable that these batch effects are due to the fact that we used mice of varying ages between experiments. Therefore, a useful future direction would be to conduct more trials of these experiments with care to keep age of the mice constant to see if this would mitigate batch effects. Additionally, analysis could be performed to determine differences in ATP production and uptake based on the age of the mice.

Once more replicates of the experiments from this study are conducted, the next steps would be to look at the effect of the mitochondria in an OGD in vitro model and in both healthy and MCAO mice. These studies would demonstrate the degree of stroke recovery that occurs after the therapeutic is administered.

Another potential future direction would be to increase uptake of mitochondria through conjugation to a microbubble. Microbubbles in combination with low pulsed focused ultrasound (FUS) treatment has been found to increase uptake of therapeutics in the brain¹⁸. Therefore, mitochondria of small particle size, such as peridroplet mitochondria, could be electrostatically conjugated to a microbubble that is then circulated with FUS treatment in order to increase uptake of the therapeutic.

An additional future direction would be to create a synthetic mitochondria. A rudimentary synthetic mitochondria, that can produce ATP in a vesicle, has been created by a research group in Germany¹⁹. Additionally, other scientists are looking to understand the mitochondria even more in order to create a more complex and holistic synthetic mitochondrion²⁰. Our current therapy proposes to harvest tissue from a patient, extract mitochondria from that tissue, and then transplant the healthy mitochondria into the damaged region of the brain. If a synthetic mitochondrion were to be created, no tissue would have to be harvested from the patient and instead the created synthetic mitochondria would be

transplanted to the damaged tissue. This method would allow for the therapy to be applied earlier and also decrease the recovery time for the patients, as they would not have to undergo tissue harvest surgery. Additionally, the synthetic mitochondria could be cultivated to have the most effective mitochondria properties and structure, such as that of peridroplet mitochondria, in order to provide the best treatment.

A final future direction for this project would be to investigate the observed difference in localization, of the different types of mitochondria, in astrocytes. The confocal z-stacks of the different types of mitochondria in the astrocytes demonstrate that each type of mitochondria localized to a different region of the cell. As seen in Figure 6A, skeletal mitochondria localized to the outskirts of the cell. In contrast, cytoplasmic mitochondria are concentrated near the nucleus of the cell. The localization of different types of mitochondria in astrocytes should be investigated and could provide insight into the differences in performance of the mitochondria in astrocytes.

Overall, this study indicated that peridroplet mitochondria is the best therapeutic option for treatment of dysfunctional mitochondria in ischemic stroke because it has high ATP production and uptake in astrocytes and harvest of adipose tissue is the most accessible and requires the least recovery of the tissue options. The use of this therapeutic method has the potential to increase recovery after stroke and reduce post-stroke complications. Therefore, these patients can have a higher quality of life, less risk of a recurrent stroke, and the ability to work. However, more trials, stroke model studies, and in vivo studies are needed to further confirm and investigate these findings and the impacts of the therapeutic on stroke recovery.

End Matter

Author Contributions and Notes

C.A.C, E.C.T, C.M.G, and R.J.P designed research, C.A.C, E.C.T, C.M.G performed research, C.A.C, E.C.T, C.M.G, and R.J.P analyzed data; and C.A.C and E.C.T wrote the paper.
The authors declare no conflict of interest.

Acknowledgments

We would like to thank Ji Song who performed all of the staining for the confocal analysis shown in Figure 6.

References

1. Yang, J.-L., Mukda, S. & Chen, S.-D. Diverse roles of mitochondria in ischemic stroke. *Redox Biol.* **16**, 263–275 (2018).
2. Roger, V. L. *et al.* AHA Statistical Update Heart Disease and Stroke Statistics-2012 Update A Report From the American Heart Association. (2011). doi:10.1161/CIR.0b013e31823ac046
3. Brown, D. L. *et al.* *Projected costs of ischemic stroke in the United States.* (2006).
4. Ciccone, A. & Valassori, L. Endovascular treatment compare to intravenous thrombolysis for acute ischemic stroke. ... *England Journal of ...* **368**, 904–13 (2013).
5. Bhatia, R. *et al.* Low Rates of Acute Recanalization With Intravenous Recombinant Tissue Plasminogen Activator in Ischemic Stroke Real-World Experience and a Call for Action. (2010). doi:10.1161/STROKEAHA.110.592535
6. Liu, F., Lu, J., Manaenko, A., Tang, J. & Hu, Q. Mitochondria in Ischemic Stroke: New Insight and Implications. (2017). doi:10.14336/AD.2017.1126
7. Hayakawa, K. *et al.* Transfer of mitochondria from astrocytes to neurons after stroke. *Nat. Publ. Gr.* **535**, (2016).
8. Robinson, K. G. *et al.* Reduced arterial elasticity due to surgical skeletonization is ameliorated by abluminal PEG hydrogel. *Bioeng. Transl. Med.* **2**, 222–232 (2017).
9. Langhorne, P. *et al.* Medical complications after stroke: A multicenter study. *Stroke* **31**, 1223–1229 (2000).
10. Ramos-Lima, M. J. M., Brasileiro, I. de C., de Lima, T. L. & Braga-Neto, P. Quality of life after stroke: Impact of clinical and sociodemographic factors. *Clinics* **73**, (2018).
11. Emani, S. M. & McCully, J. D. Mitochondrial transplantation: applications for pediatric patients with congenital heart disease. *Transl. Pediatr.* **7**, 169–175 (2018).
12. Huang, P.-J. *et al.* Transferring Xenogenic Mitochondria Provides Neural Protection against Ischemic Stress in Ischemic Rat Brains. *Cell Transplant.* **25**, 913–927 (2016).
13. Huang, J. L., Manaenko, A., Ye, Z. H., Sun, X. J. & Hu, Q. Hypoxia therapy-A new hope for the treatment of mitochondrial dysfunctions. *Medical Gas Research* **6**, 174–176 (2016).
14. Benador, I. Y. *et al.* Mitochondria Bound to Lipid Droplets Have Unique Bioenergetics, Composition, and Dynamics that Support Lipid Droplet Expansion. *Cell Metab.* **27**, 869–885.e6 (2018).
15. Miller, F. J., Rosenfeldt, F. L., Zhang, C., Linnane, A. W. & Nagley, P. Precise determination of mitochondrial DNA copy number in human skeletal and cardiac muscle by a PCR-based assay: lack of change of copy number with age. *Nucleic Acids Res.* **31**, 61e–61 (2003).
16. Park, S.-Y. *et al.* Cardiac, skeletal, and smooth muscle mitochondrial respiration: are all mitochondria created equal? *Am. J. Physiol. Heart Circ. Physiol.* **307**, H346–52 (2014).
17. Boengler, K., Kosiol, M., Mayr, M., Schulz, R. & Rohrbach, S. Mitochondria and ageing: role in heart, skeletal muscle and adipose tissue. *Journal of Cachexia, Sarcopenia and Muscle* **8**, 349–369 (2017).
18. Gorick, C. M. *et al.* Sonoselective transfection of cerebral vasculature without blood-brain barrier disruption. *Proc. Natl. Acad. Sci. U. S. A.* **117**, 5644–5654 (2020).
19. Göpflich, K., Platzman, I. & Spatz, J. P. Mastering Complexity: Towards Bottom-up Construction of Multifunctional Eukaryotic Synthetic Cells. *Trends in Biotechnology* **36**, 938–951 (2018).
20. Biner, O., Schick, T., Ganguin, A. A. & Von Ballmoos, C. Towards a synthetic mitochondrion. *Chimia (Aarau).* **72**, 291–296 (2018).